GFRP Reinforced High Performance Glass–Bolted Joints: Concept and Experimental Characterisation

Mithila Achintha

School of Engineering, University of Southampton, Southampton, SO17 1BJ, UK

E-mail: Mithila.Achintha@soton.ac.uk (Corresponding Author)

Tudor Zirbo

School of Engineering, University of Southampton, Southampton, SO17 1BJ, UK

E-mail: tdz1u16@soton.ac.uk

Abstract

This paper presents the results of an experimental investigation into the use of externally-bonded Glass Fibre Reinforced Polymer (GFRP) strips as a means of improving the load capacity and delayed failure characteristics of glass-bolted joints. The peak load and the failure behaviour of GFRP reinforced bolted joints in annealed, heat-strengthened and tempered glass were investigated using the experiments of double-lap tension joint configurations. The results were compared with that of reference unreinforced joints, and bolted joints in commercially available laminated-annealed glass. The paper shows that GFRP reinforcement ensured significantly enhanced structural performances of the joints in annealed and heat-strengthened glass. Although the bolted joints in tempered glass showed the highest load capacity, the joints failed with no ductility where tempered glass shattered into small dices.

Keywords:

Bolts, Ductility, Experiments, Glass, Joints, Load capacity

1. Introduction

By combining recent advances in glass products (e.g. low-emissivity, solar control, photovoltaic, etc.) with building physics (e.g. passive ventilation, solar energy, etc.) and digital designs (e.g. BIM, prefabrication), it is possible to tailor energy-efficient buildings, whether concentrating daylight and/or capturing the sun's energy [1]. However, exploitation of full potential of glass in buildings is currently being held back by the inefficiency of the contemporary glass-joint techniques because of the low tensile strength and brittle material behaviour of glass [2]. Joints mostly govern the overall design of glass structures/panels and hence, structurally inefficient joints result in inefficient structures. Traditional frame-supported glazing systems are unable to meet the modern structural and aesthetic requirements because of their limited use in load-bearing applications/novel geometries, and due to the additional weight and visual impact [3]. Adhesive bonding has the potential for mounting glass panels [4], but the limited knowledge and the uncertainty regarding durability and long-term structural behaviour mean that the industry has reservations about the use adhesive joints in civil engineering structures [5].

Mechanical fixing methods, essentially various forms of bolted connections, are increasingly used in modern glass construction because of their "frameless" characteristics. Both bearing and friction-based bolted connections are currently used in glass construction [6]. In addition to the use of standard cylindrical bolts [7], countersunk [7] and articulated bolts [8] are also used as means of ensuring rotational freedom in out-of-plane directions. Provision of safe and reliable joints in glass structures is increasingly difficult, since glass in the vicinities of the connectors subject to complex states of high stress concentrations, including additional forces/stresses due to the movements and dimensional tolerances of the structures [8]. The local stress concentrations developed in glass due to the contact with the bolts cause further concentrations of high stresses around the bolt holes. Although isolating bolts from glass via the use of more compliant materials such as aluminium, mortar and plastics, all of which are known to redistribute the stresses and reduce the effects of localised contacts to a certain extent, glass still fails in brittle manners in the vicinity of the joints [9].

The tensile strength of annealed glass (i.e. basic float glass) is ~40 MPa [8]. Due to the presence of surface flaws/defects in drilled holes, the actual tensile strength of glass in the vicinity of a bolted joint can be lower than that specified by the glass manufacturers. The low tensile strength of annealed glass mean bolted joints are not usually used in practice to connect annealed glass panels to adjacent panels or supporting structures. In construction industry, thermally strengthened glass is used when bolted joints are required. Owing to the surface compressive prestresses developed in glass as a result of thermal strengthening, fully strengthened glass (also known as tempered glass or toughened glass) and partially-strengthened glass (also known as heat-strengthened glass) have higher apparent surface tensile strength compared to annealed glass. Usually, surface compressive prestresses of magnitude 80–150 MPa and 24–52 MPa are present in tempered and heat-strengthened glass, respectively [8].

Despite the high strength of thermally strengthened glass compared to annealed glass, the former is significantly more expensive compared to the latter. Furthermore, additional thermal treatments mean that the embodied energy impact of thermally strengthened glass is higher compared to that of annealed glass [10]. The major engineering limitation associated with the use of tempered glass is that they fail into very small pieces with no residual load capacity after the initiation of a fracture [11]. Sizing, drilling, cutting etc. of thermally strengthened glass are difficult, and hence the processing steps are usually done prior to thermal strengthening. The low degree of strengthening around holes in tempered glass [12] also limits the actual benefit of thermal strengthening in glass-bolted joints applications.

Commercially available laminated glass, which are produced by combining two or more glass sheets with one or more thin PolyVinylButyral (PVB) polymer or ionomer interlayers, are usually preferred in industry as a means of ensuring safe failure behaviour compared to monolithic glass. However, squeezing of the polymer interlayers due to the pressure exerted on glass in the vicinity of the joints can limit the effectiveness of the use of laminated glass [2]. Low strength capacity of the interlayers also means the ability for it to ensure a high post-cracked load resistance is limited. Laminated glass is expensive compared to monolithic glass and the processing steps such as cutting and drilling holes must be carried out before the lamination.

The inefficiency of the contemporary glass-bolted joint techniques and the lack of confidence in current design methods mean that joints are typically overdesigned with high safety factors, leading to excessive material usage as well as added weight and cost [2]. Inefficient joint techniques have prevented generic exploration of the structural glazing applications. Some research works [13,14] reported in the literature attempted advancement of the glass–bolted joint techniques; mostly the comparative performance of different bushing/isolating materials and geometric characteristics such as closeness of the fit (i.e. the bolt diameter relative to the hole diameter) of the joints. However, these studies were limited to tempered glass and no genuinely structurally efficient joint technique was developed. There is a need for structurally efficient and reliable glass-bolted joint techniques in order to enable the full potential of glass as a construction material. In particular, a technique that is practically feasible for annealed glass, where availability, low cost/embodied energy, easy constructability, prospect for post-cracked load resistance, etc. of annealed glass mean it is a better construction material compared to tempered or laminated glass.

A previous research investigation [15, 16] led by the first author of the present paper showed the potential of adhesively bonded thin GFRP strips to reinforce annealed glass in the vicinity of a hole geometry. The reinforced annealed glass ensured higher load capacity and notable post-cracked load resistance compared to the reference unreinforced glass. The present paper extends the findings of the previous work [15, 16] and experimentally explores the concept of GFRP reinforcement as a means of ensuring enhanced structural performance of double-lap tension bolted joint configurations in annealed and heat-strengthened glass. Whilst the technique proposed in the present paper or other similar strengthening methods are not reported in the literature for glass–bolted joints, adhesively bonded fibre-metal laminates strips have been successfully used in aircraft structures as a means of improving damage tolerance through their contributions as a bonded crack retarder [17]. Given glass is a brittle material and glass fractures in the vicinity of the bolted joints, it is expected that the crack retardation contributions of the bonded GFRP strips will enhance the structural response of the glass-bolted joints.

2. Materials

2.1 Glass

The load response and the failure behaviour of bolted joints in commercially available annealed, heat-strengthened, tempered and two-layer laminated-annealed glass were investigated in the present study.

2.1.1. Residual stress in glass

The residual stress (i.e. initial stress) in the different glass types were measured using a scattered-light-polariscope, SCALP-05 [18, 19]. SCALP-05 uses glass birefringence that changes the polarisation of an input laser beam and the consequent variation in the optical retardation of the scattered light to determine the stress at a given location of glass. Fig. 1 shows the use of SCALP-05 to measure the surface residual stress in a glass specimen.

Figure 1: Use of SCALP to measure surface residual stress in glass

In the experiments, the surfaces of the glass specimens were first cleaned to remove dirt and fingerprints, and the residual stresses were then measured by placing the polariscope at middle region of the glass specimen. The polariscope was connected to an integrated software via a computer where the software processed and displayed the residual stress measurement data. A good optical contact between the glass sample and the polariscope was ensured by using a SCLAP-manufacture-recommended oil-based immersion liquid (refraction index = 1.52) [19]. The measurements were repeated a few times (usually about six times) at the same location in order to achieve consistent results. Details of the use of SCALP-05 to measure stresses in glass can be found in elsewhere [18, 20, 21, 22]. Table 1 shows the measured average surface compressive residual stress in all glass types investigated in the present study. The measured surface residual stress data agree with the surface residual stress values determined in the experimental investigations as well as the typical value ranges specified by European Standards. For example, surface residual stress values of magnitude less than 10 MPa were reported in annealed glass [23], whereas BS EN 1863 [24] states the surface precompression stress in heat-strengthened glass must be within the range 24 MPa to 52 MPa. According to BS EN 12150 [25], the surface compressive residual stress in tempered glass must be in the range 80 MPa to 150 MPa.

Table 1: Measured surface compressive residual stress in different types of glass

Glass type	Surface (compression) residual stress (MPa)
Annealed	~5
Heat-strengthened	~30
Tempered	~95
Laminated annealed glass	~3

2.2. Glass Fibre Reinforced Polymer (GFRP) reinforcement

The GFRP strips that used to reinforce the glass-bolted joints were made by impregnating commercially available unidirectional 'E-glass' dry fabric using a commercially available twopart epoxy resin – EL2 epoxy laminate resin with AT30 slow hardener [26] – in a wet lay-up method. The GFRP was cured in ambient conditions for minimum of seven days. The ultimate tensile strength, the Young's modulus and the Poisson's ratio of a similar GFRP used in a previous research [27] were determined to be 450 MPa, 24.5 GPa and 0.18, respectively. In the present study, all glass–bolted joints test specimens failed due to glass fracture. No GFRP failure or the glass–GFRP bond failures were observed in the experiments. However, a detailed investigation is proposed for a future investigation in order to analyse the effects of adhesive and GFRP in more detail, together with potential premature failure of the adhesive and/or the interfaces prior to glass fracture.

2.3 Adhesive

Epoxy adhesive "Araldite 2020" [28] was used in the present study to bond the GFRP strips onto the glass specimens. Based on an experimental investigation [27] on early strength gain of this adhesive, it was determined to cure the adhesive in an autoclave at 40^{o}C for 24 hours, followed by further curing in ambient conditions for six days in order to achieve a satisfactory glass–GFRP bond in the reinforced glass-bolted joints. The results of the present experimental investigation showed no premature adhesive or bond failures prior to the glass fracture. This suggests that the curing process used in the present study ensured appropriate strength in the adhesive and the glass–adhesive and adhesive–GFRP interfaces. Using uniaxial tensile tests carried out in accordance with ASTM D638-02 [29], the Young's modulus within the initial approximately linear stress-strain response, the ultimate tensile strength and the strain of the adhesive were determined to be ~3GPa, ~45 MPa and ~0.037, respectively.

3. Glass-bolted joints test specimens

Reference (i.e. unreinforced) glass-bolted joints test specimens of annealed, heat-strengthened, tempered and laminated-annealed glass, and reinforced glass-bolted test specimens of annealed, heat-strengthened and tempered glass were fabricated and tested in the present study (Table 2). No reinforced laminated glass test specimen was prepared or tested in the present study, since it was decided to investigate the effectiveness proposed glass–bolted joint strengthening technique against the joints in commercially laminated glass, which are currently used in building construction industry as structural glass (i.e. load-bearing) applications.

Table 2: Types of glass-bolted joints tested in the study

Glass type	Reference glass-bolted joint	Reinforced glass-bolted joint
Annealed	Yes	Yes
Heat-strengthened	Yes	Yes
Tempered	Yes	Yes
Laminated annealed	Yes	No

3.1. Reference (i.e. unreinforced) glass–bolted joints test specimens

As shown in Fig. 2, a double-lap tension test geometry was used in the present study to test both unreinforced and reinforced glass-bolted joints. The double-lap tension joint geometry was used because of its potential for applying a uniaxial tension load on the glass whilst eliminating eccentric loading on the bolted joints.

The glass-bolted joint was fabricated by fixing two glass sheets using two M10 bolts at each end of the glass specimens. It was decided to use M10 bolts, since M10 bolts are commonly used in construction industry. Since fixing glass specimens directly into the loading grips of the test machines is likely to cause premature failure of glass in the vicinity of the loading grips, it was decided to use aluminium alloy plates to fabricate glass-aluminium bolted joints, and then fix the aluminium alloy plates into the test machine (see Fig. 2). An aluminium alloy was chosen because of their similar Young's modulus to that of glass (~70 GPa) and its ductile material behaviour, which ensured no premature failure in the fixing areas.

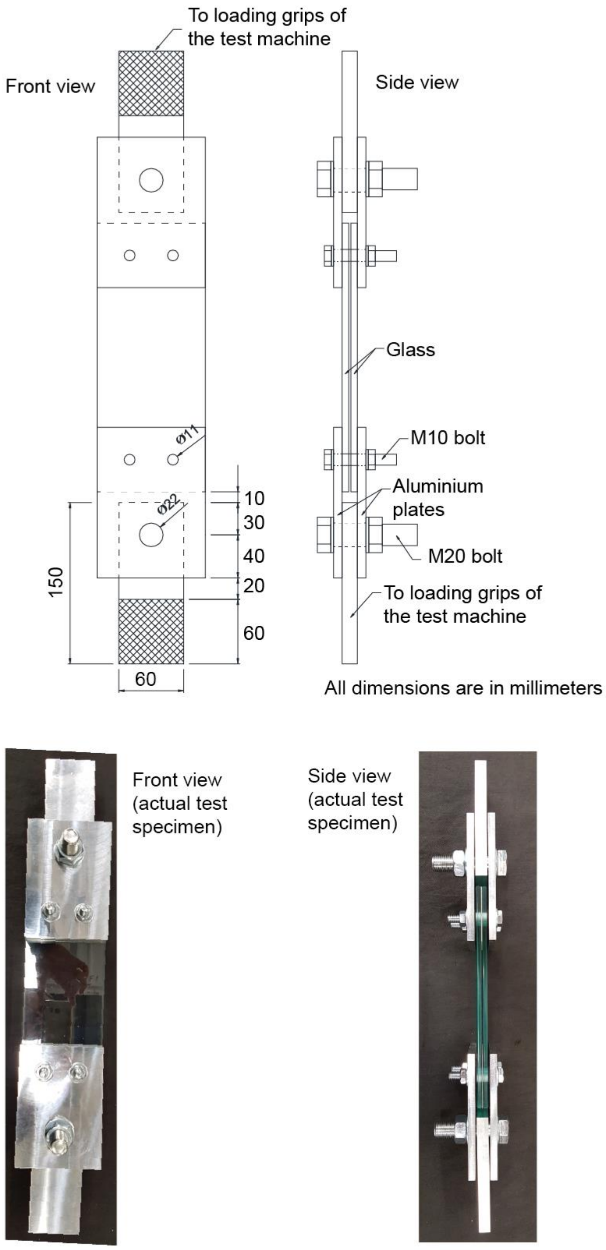

Figure 2: Reference (i.e. unreinforced) glass-bolted joint test specimen

In order to minimise the effects due to possible rotations of the test specimen/loading grips, the test specimens were loaded through a pinned joint rather than directly fixing the aluminium alloy plates into the loading machine (see Fig. 2). This was done by first connecting the free-ends of the aluminium alloy plates to another thick aluminium alloy plate using a M20 bolt at each end of the test specimen. The free-ends of the two thick aluminium plates were then fixed to the loading grips of the test machine (see Fig. 2).

3.1.1. Geometric details of the glass specimens

By considering the minimum size of heat-strengthened, tempered and laminated glass that can be easily purchased from commercial glass suppliers, it was decided to use 250 mm (length) x 100 mm (width) and x 6 mm (thickness) glass specimens. It should be noted that, due to the presence of the PVB interlayer the actual nominal thickness of the two-layer laminated annealed-glass was ~6.4 mm (two glass sheets (each 3 mm thick) and the thickness of the PVB interlayer).

In order to fix two M10 bolts at each end of the glass specimens, two holes were drilled at each end as shown in Fig. 3. The location of the bolt holes with respective to the adjacent edges and corners and the size of the hole compared to the bolt size are important design parameters. However, there are no widely accepted guidelines among the glass engineering research and industry communities. It was decided to drill holes of 11 mm diameter as a means ensuring some space for inserting a rubber layer as an isolating material between the internal surface of the hole and the surface of the bolt shank. IStructE guidelines on "Structural Use of Glass in Buildings" [8] recommend no holes should be drilled within distance 2*t* (*t*- thickness of the glass, which was 6 mm in the present study) from any edge, and within distance 4*t* from a corner. In the present study, the holes were drilled such that the centre of each hole was 30 mm from the adjacent edges of the glass specimen (see Fig. 3). The location and the size of the hole ensured clear distances of 24.5 mm (i.e. > 2*t*) from an edge and 36.9 mm from the corner (i.e. >4*t*), respectively.

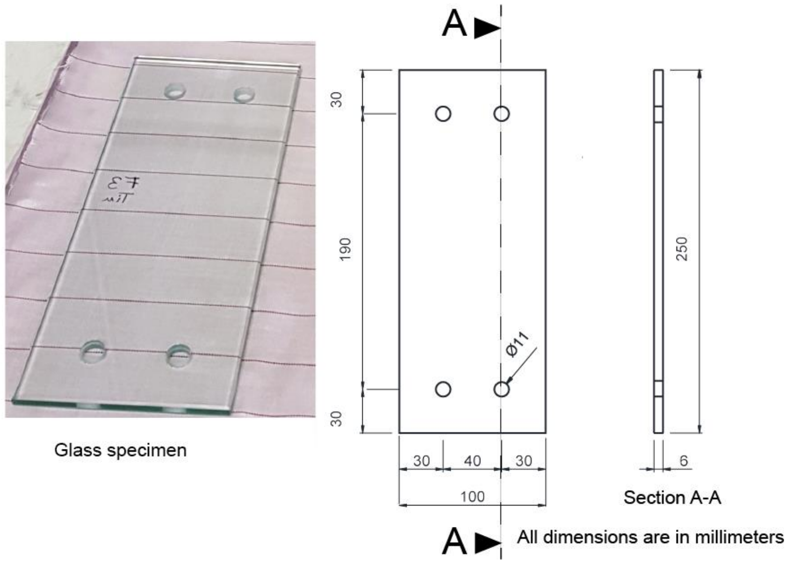

Figure 3: Geometry and dimensions of the glass specimens

Services of a commercial supplier was used to cut the glass specimens into the specified size and to drill the holes. In heat-strengthened and tempered glass, the holes were drilled prior to the thermal strengthening processes. In order to ensure that the experiments were carried out mimicking relevant practical industrial applications, all edges and the inner surfaces of the drilled holes of the glass specimens were polished up to the “industry standard” by the commercial supplier. The distributions and the sizes of the surface/edge defects measured using an optical microscope were largely similar in all specimens. Only a few surface defects were present in the vicinity of the drilled holes. The defects were measured to be around ~50 μm in size. Therefore, as a starting point, it was assumed that the experimental results of the overall load response and the failure behaviour of different test specimens may be compared with the assumption that the effects of edge/surface flaws were similar in all glass specimens.

3.1.2. Details of the aluminium alloy plates

Fig. 4a shows the dimensions of the aluminium alloy plates that used to fabricate the joints. Aluminium alloy 6082 T6 (yield stress = 255 MPa) was used in the present study. The width (100 mm) and the thickness (6 mm) of the aluminium plates were chosen to be the same as that of the glass specimens. Similar to the glass specimens, two 11 mm diameter holes were drilled at each end of each aluminium alloy plate specimens as shown in Fig. 4. In order to ensure the alignment with the glass specimens in the glass–bolted joint test specimens, the holes were drilled such that centre of each drilled hole was 30 mm from the two adjacent edges. The length (140 mm) of the aluminium plate were sufficient to fix the test specimens into loading grips of the test machine using the method described below (see Section 3.1.3).

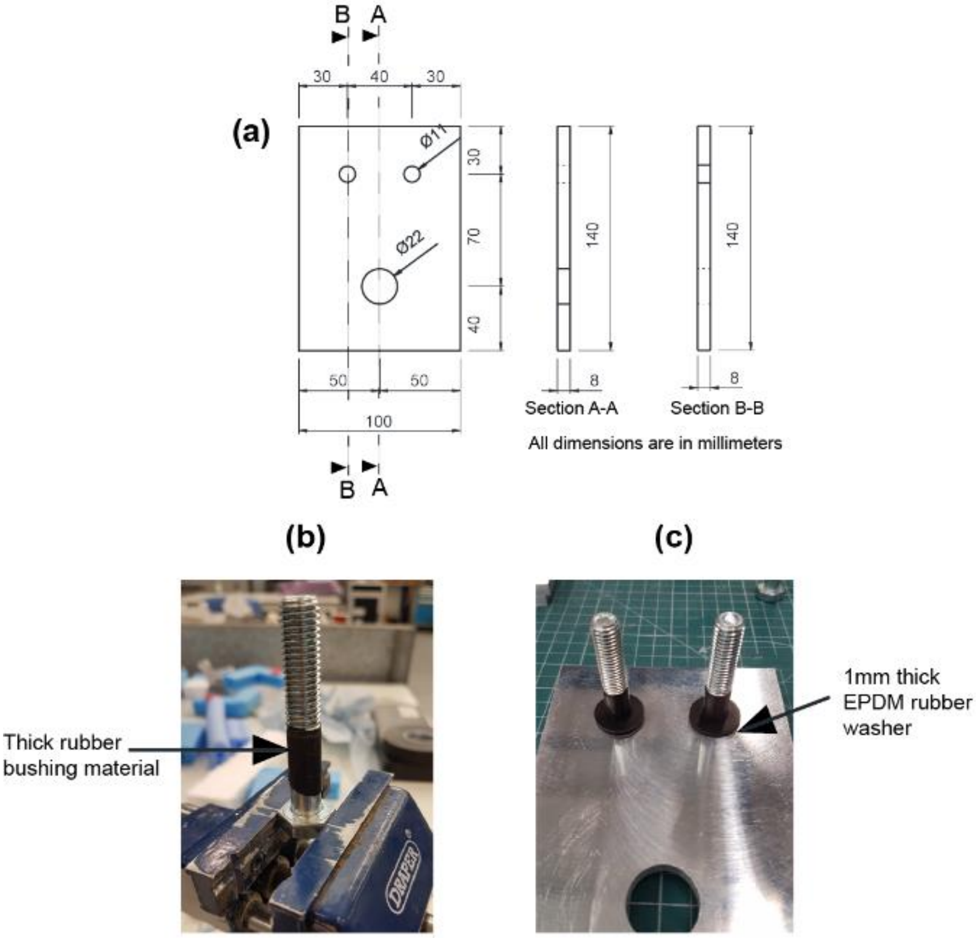

Figure 4: (a) Geometry and dimensions of the Aluminium alloy plate, (b) rubber bushing, (c) rubber washers

3.1.3. Fabrication of the reference glass–bolted joints

Firstly, one glass specimen was kept on the top of another glass specimen such that the relevant holes in the two glass specimens were aligned with each other. Then, an aluminium alloy plate each placed on outer side of the two glass specimens at both ends with correct alignment of the holes of the two glass specimens. Class 5.6 (nominal yield stress ~ 300 MPa [30], M10 (diameter ~10 mm) steel bolts were used to connect the glass specimens and the aluminium plates. In order to eliminate the direct contact with the steel bolt and the inner surfaces of the holes in the glass specimens, a thick rubber was used as a bushing material (see Fig. 4b). EPDM rubber washers of ~1 mm thick were used to avoid direct contact between the glass and the aluminium alloy plates (see Fig. 4c). The current design was used because of its convenience for fabrication and testing. The experimental results suggested no premature bolt failure prior to the glass fracture.

In order to ensure the same geometric details in both unreinforced and reinforced glass-bolted joints, a few small pieces of GFRP which were cut from the same GFRP that used for the reinforced joints were sparsely distributed between the two inner sides of the two glass specimens in the reference glass–bolted joints. These small pieces of GFRP were not bonded to glass in the reference joints, but just held in place due to the pressure exerted on them due to the of bolts. The GFRP spacers did not contribute to the load response or the failure behaviour of the unreinforced joints but ensured the alignment of the glass pieces prior to the test and enabled the use of same end aluminium plates in both unreinforced and reinforced glass–bolted joints. The thick end aluminium plates were ~15.35 mm thick and fitted within the free space between the two 6 mm thick aluminium plates (i.e. 2 x 6mm + 2 mm (total thickness of the two washers) + 1.35 mm (thickness of the GFRP) = 15.35 mm).

All bolts were snug-tight with no pretensioning in the bolts. Pretensioning in the bolts can be decisive for the performance of the bolted joints. However, the present study focused on the performance of snug-tight bolts only; there is a scope for a future study on investigation of reinforced glass–bolted joints with pretensioned bolts. Reference (i.e. unreinforced) glass-bolted joint specimens were fabricated for annealed, heat-strengthened, tempered and laminated-annealed glass.

3.2. Reinforced glass-bolted joints test specimens

Reinforced glass-bolted joint test specimens were prepared in the same way as the reference unreinforced test specimens (Section 3.1). However, GFRP strips (Section 2.2) were bonded between the two glass sheets at both ends of the glass specimens.

3.2.1. Geometric details of the GFRP strips

The average thickness of the used cured GFRP laminate was ~1.35 mm. The GFRP strips (see Fig. 5) were cut into the size of 60 mm (length) x 100 mm (width) using a circular diamond saw. The width of the GFRP (100 mm) was chosen to be the same width as the glass specimen and the length 60 mm was assumed to be sufficient to reinforce the glass around the bolted joints at each end of the glass specimens. The length of the GFRP strip can be decisive for the performance of the reinforced joints. The optimal length of the GFRP strip may be determined from a detailed stress analysis of the joint. However, in the present “proof of concept study”, an arbitrary length was chosen such that the visual impact of glass was not significantly affected by the presence of a small area of translucent GFRP. In order to use the GFRP strips in the bolted joint configurations, two 11 mm diameter holes were drilled in each GFRP strip. In order to ensure alignment with the glass specimens in the reinforced glass–bolted joint test specimens, the holes were drilled such that centre of each drilled hole was 30 mm from the two adjacent edges (see Fig. 5 for details).

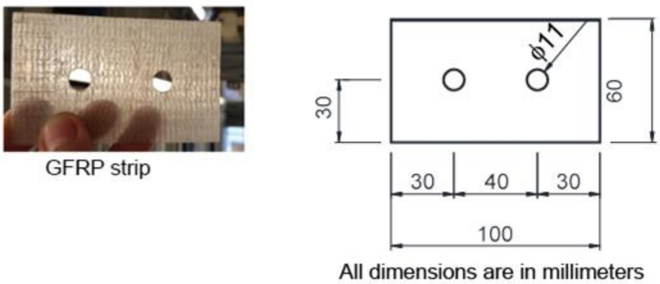

Figure 5: Geometry and dimensions of the GFRP reinforcement

After the concept of GFRP reinforcement has validated in this paper, there is a scope for a future work on detailed experiment and computational investigation based on strain/displacement evolution and likely failure modes for the development of a comprehensive design methodology for GFRP reinforced glass-bolted joints. Existing research investigations on progressive failure simulation and experimental validation of bolted joints in Fibre Reinforced Polymers (FRP) materials (e.g. [31]) and the evolution of fracture in brittle and quasi-brittle solids (e.g. [32]) provide useful background for the development of the future computational framework for the analysis and design of GFRP reinforced glass-bolted joints.

3.2.2. Fabrication of reinforced glass–bolted joints

Prior to the bonding of the GFRP strips, all bonding surfaces of the GFRP and the glass were thoroughly cleaned and degreased using acetone. Previous research [20, 27] involving glass and the same GFRP and adhesive showed that bond lines of ~0.1 mm thick ensured no premature bond failures when the test specimens were loaded after seven days of curing. The same bond line thickness and the curing procedure were used in the present study.

It was decided to bond the GFRP strip on inner sides of the two glass specimens in the joint, since bonding of GFRP strips on outer sides of glass is less likely a practically viable option given visual and physical constraints that may cause. The volume of the adhesive required to obtain a ~0.1 mm thick layer was evenly spread using a spatula over the bond surfaces of both glass specimens. The viscosity of the adhesive was sufficient to apply the adhesive on the surfaces of the horizontally orientated glass specimens. One side of the GFRP strip was then placed on the top of one glass specimen whilst ensuring right alignment with the holes and the edges. The bonding was done carefully whilst ensuring no air bubbles were trapped in between by applying a light pressure by gently pressing the parts together. After initial hardening of the adhesive bond (the pot life of this adhesive was about 30 minutes), the second glass specimen was placed on the top of the other side of the GFRP strip with the correct alignment. Once the adhesive bonds have hardened enough, the specimens were then secured safety using small clamps while ensuring no exerting pressure on the initially set adhesive. The specimen was then cured in an autoclave at 40º C for 24 hours, followed by further curing in ambient conditions for six days in order to achieve a satisfactory glass–GFRP bond in the reinforced glass-bolted joints. Fig. 6a shows the adhesively bonded GFRP reinforcement strip at one end of a double-layer glass specimen, and Fig. 6b shows a schematic view of a reinforced glass-bolted joint configuration.

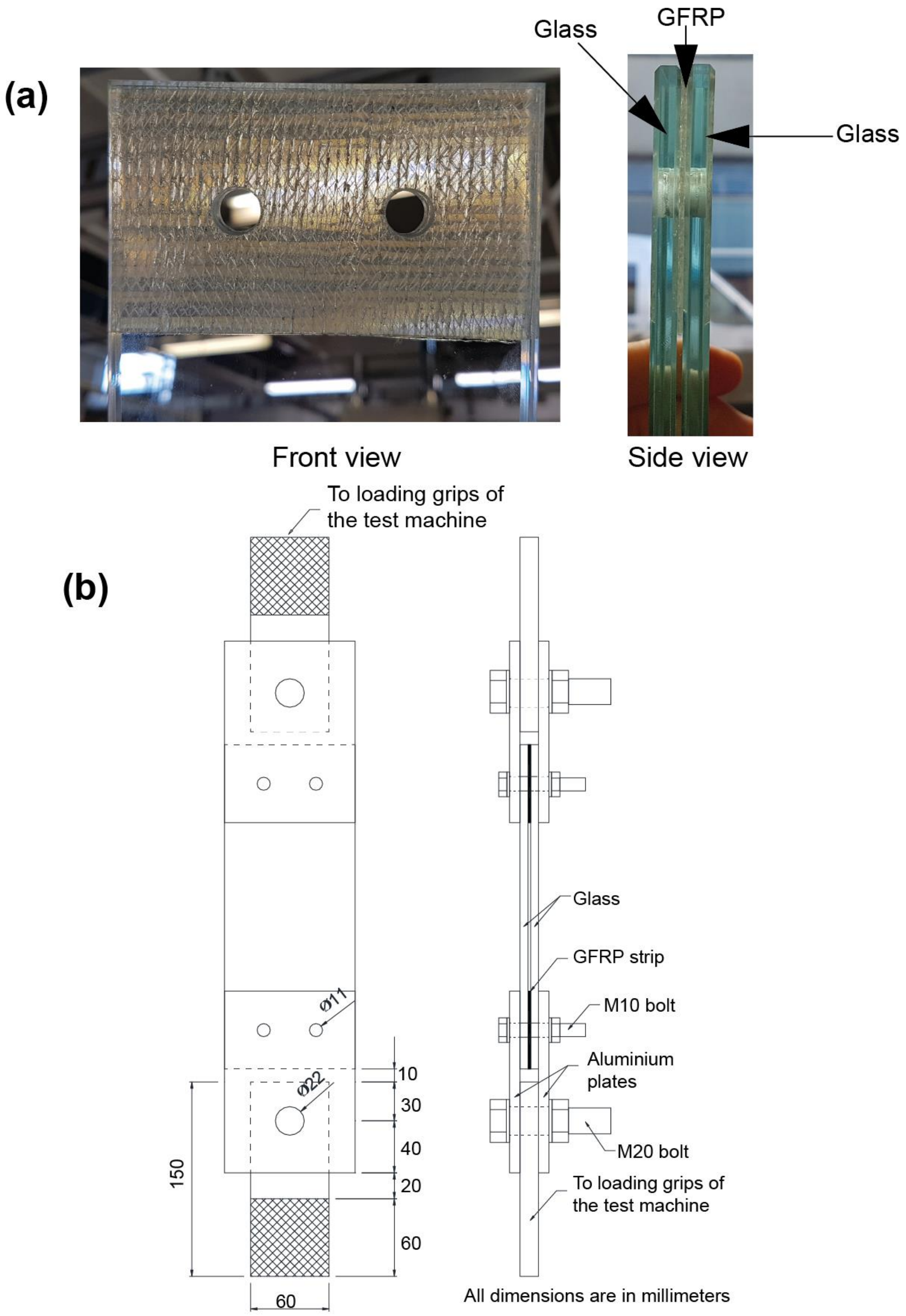

Figure 6: (a) GFRP reinforcement in the vicinity of the bolted joints, (b) reinforced glass-bolted joint configuration

Table 3 summaries all key geometric details of the components of the test specimens.

Table 3: Geometric details of the test specimens (note: *l* – length, *w* – width and *t* – thickness)

Glass specimens			GFRP strips			Aluminium plate			End aluminium plate		
l (mm)	*w* (mm)	*t* (mm)	*l* (mm)	w (mm)	*t* (mm)	*l* (mm)	*w* (mm)	*t* (mm)	*l* (mm)	*w* (mm)	*t* (mm)
250	100	6	60	100	1.35	140	100	6	150	60	15.35

4. Test arrangement

Three specimens from each test category were tested in the present study. Electronic levels and digital inclinometers were used to align the test specimens with the direction of the loading grips as a means of ensuring exact alignment between the line of action of the applied force and the test specimen. Testing was carried out displacement controlled at a slow rate (1 mm/min), which was deemed to be a representative of a realistic quasi-static load. Since there are no widely accepted test standard for testing glass, the displacement rate of 1 mm/min was chosen based on the previous experience of the authors [20, 27]. A servo-hydraulic test machine Schenck 630, which is available in the Testing Structures Research Laboratory at the University of Southampton was used to test the glass-bolted joints. This test machine loaded the test specimens in tension where one end of the test machine (bottom end grips) moved whilst the other end (top end) remained stationary. Fig. 7 shows a glass–bolted joint test specimen fixed to the test machine.

Strain data along the loading direction of the glass test specimens were recorded using two linear strain gauges fixed at middle regions of the two outer glass surfaces (see Figure 7 for the location of the strain gauges). Tests were continued until the failure of the test specimens whilst the load and strain gauge data were continuously recorded using software associated with the test machine.

Figure 7: A glass–bolted joint test specimen fixed to the test machine

5. Experimental results

For brevity, only the detailed results of one test specimen from each category are presented in this paper while the recorded maximum load of all test specimens are also provided. The presented results are representative of all test specimens of the respective test specimen category. All observed maximum loads were within ±15% of the average failure load of the respective category of the glass–bolted test specimens. This range is within the scatter of test results usually reported (about 20% variance) in the literature (e.g. [33]) for test results of glass test specimens. A detailed statistical analysis such as standard deviation and coefficient of variation was not performed in the present study given such an analysis may be of less value, since only three test specimens from each test category were tested.

Although the longitudinal strain data were recorded in the middle regions of the glass specimens, these data were not able to investigate the development of stress concentrations in the vicinity of the bolted joints. Therefore, the strain gauge data measured in the middle regions of the glass specimens were not used in this paper for the comparisons between the load response and the failure behaviour of the glass-bolted joints test specimens. Similarly, the displacement data recorded based on the movement of the crosshead of the test machine which included initial slip occurred in the test specimens prior to a proper contact was established between the bolt and the glass, were also not used for detailed analysis. The initial slip could depend on several local factors which were not explicitly monitored in the present study. Therefore, comparisons based on the available displacement data would inherently include different initial slips, which were of the same order of magnitude as the reported overall displacements and could hamper accurate comparisons between different test specimens.

The objective of this paper is an experimental validation of the enhanced load capacity and delayed failure of the GFRP–reinforced glass–bolted joints in annealed and heat-strengthened glass. Therefore, it was decided to present the results of the glass–bolted joint test specimens as load vs time graphs. These graphs represent what actually happened in the experiments and ensure comparisons free of additional uncertainties.

5.1. Annealed glass-bolted joints test specimens

5.1.1. Reference (i.e. unreinforced) annealed glass-bolted joints test specimens

The reference annealed glass-bolted joint test specimen failed due to major cracks developed in the vicinity of the bolted joint. The cracks caused a completed failure of the glass across the bolted joint; however, middle regions of the glass specimens (i.e. away from the bolted joint) remained intact (see Fig. 8a). The dotted line in Fig. 8b shows the load response of the reference annealed glass test specimen. It can be noted from the figure that during an initial time period of ~80s, no significant force was applied on the test specimen. This is due to the displacement required to establish an appropriate contact between the bolt shanks and the glass/aluminium plates to activate the bearing forces. By combining the results shown in Fig. 8b together with the visual/audio observation made during the test, it was determined that one glass specimen failed at the applied load ~3920 N (reported maximum load for other two specimens were 3760 N and 4340 N) (average maximum load – 4007 N) and the load resistance was dropped to ~2440 N instantaneously. The remaining intact glass specimen then carried the load briefly for about few seconds where the load resistance was increased up to ~3420 N. However, at this load the second glass specimen also failed and the load resistance of the joint was lost instantaneously causing a complete brittle joint failure (Fig. 8b).

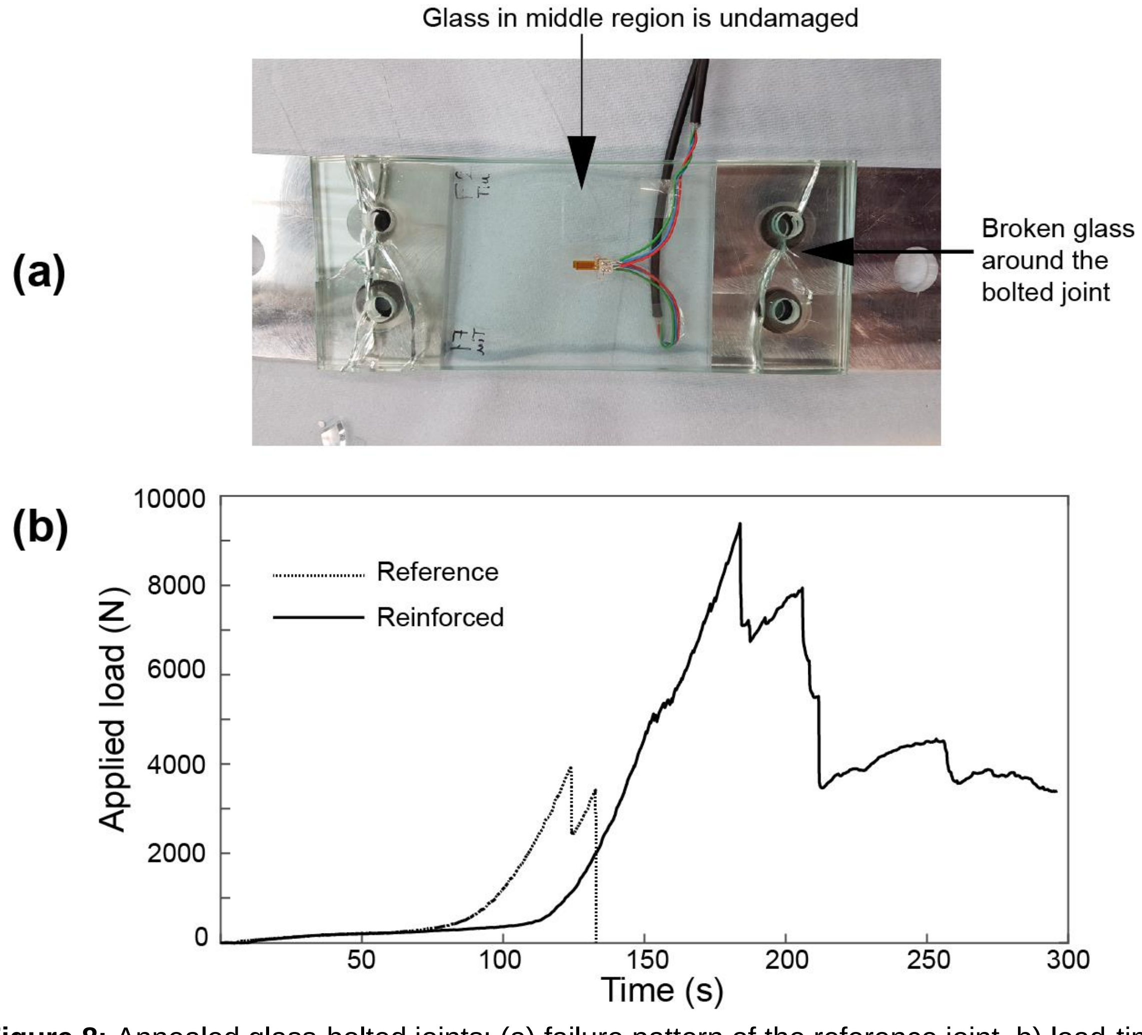

Figure 8: Annealed glass-bolted joints: (a) failure pattern of the reference joint, b) load-time relationships of the reference and reinforced joints

5.1.2. Reinforced annealed glass-bolted joint test specimens

The solid line in Fig. 8b shows the load response of the reinforced annealed glass-bolted joint test specimen. The analysis of the results shown in the figure and the audio observations made during the test suggest that microcracks started to develop in the joint area at applied load ~5100 N. However, unlike the reference test specimens, the reinforced joint did not fail instantaneously after the initiation of cracks in glass but continued to carry the applied load. The maximum load resistance of the joint was ~9400 N (reported maximum load for other two specimens were 9100 N and 10810 N) (average maximum load – 9770 N). The initial phases of the load response of the joints (i.e. prior to the development of bearing forces) depended on local details such as the closeness of fit and the geometry of the bushing materials.

As shown in Fig. 9a, glass in the reinforced joint too failed in the vicinity of the bolted joints. However, unlike a single major crack that caused the failure of the reference annealed glass –bolted joints, many cracks resulting in small glass fragments caused failure of the reinforced annealed glass-bolted test specimen (see Fig. 9b). The GFRP strip held the broken glass pieces together and hindered the development /propagation of a dominant crack. Similar to the reference glass-bolted joints test specimens, after the failure of one of the glass specimens, a drop in the load resistance was noted and then the second glass specimen resisted the applied load for a brief period. The second glass specimen of the reinforced bolted joint failed at ~7950 N. However, unlike the reference annealed glass-bolted joint where the load resistance instantaneously dropped to zero after the failure of the second glass plate, the reinforced joint resisted some load (~3400–4570 N, see Fig. 8b), albeit a lower resistance compared to the uncracked reinforced joint. Fig. 9c shows the GFRP strip and the glass specimen after the broken small glass pieces were removed after the test specimen was taken out of the test machine. The visible deformation of the GFRP suggested that the GFRP strip carried the load after the glass had failed in the vicinity of the bolted joints.

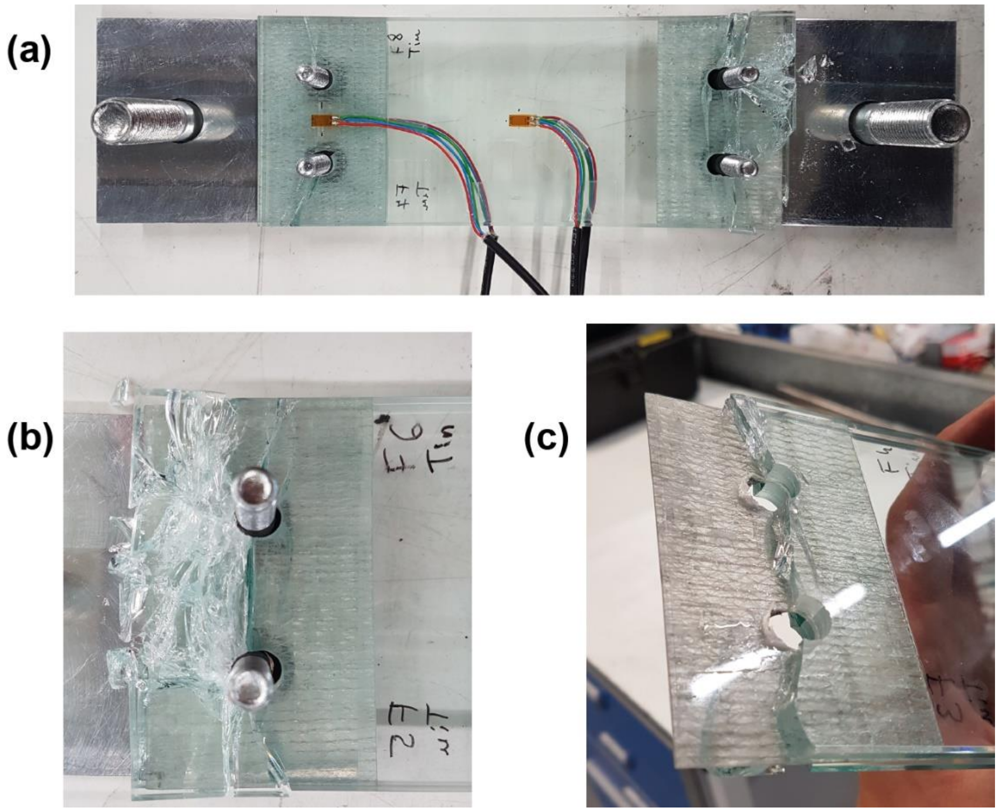

Figure 9: Reinforced annealed glass test specimen: (a) failure pattern, (b) glass failure in the vicinity of the bolted joint, (c) vicinity of the bolted joint after the broken glass pieces were removed

5.1.3. **Strain data in reference and reinforced annealed glass-bolted joints specimens**

Figs. 10a and 10b show the strain data recorded on each outer side of the glass test specimens at middle regions of the reference and reinforced annealed glass-bolted joints test specimens, respectively. The recorded strain gauge data on the two outer surfaces of a given test specimen were reasonably similar and showed similar relationships with the applied load. The results suggest that the test specimens did not experience significant bending and hence, as expected, largely a uniaxial tension force was applied on the glass specimens. It is also believed that applying the load through pinned connections ensured that the test specimens were able to adjust small deviations/movement of the loading grips in directions perpendicular to the applied load. Strain data recorded in all other test specimens investigated in the present study were qualitatively similar to the results shown in Fig. 10. The results shown in Fig. 10 also suggest that similar strains values were recorded in both reference and unreinforced glass-bolted joints within the load range of the reference joint. It is believed that since the

GFRP strips were thin compared to the substrates of the joints (i.e. glass and aluminium), the contribution of the GFRP reinforcement to the axial stiffness of the reinforced joint within the pre-cracked regime of the glass was not significant.

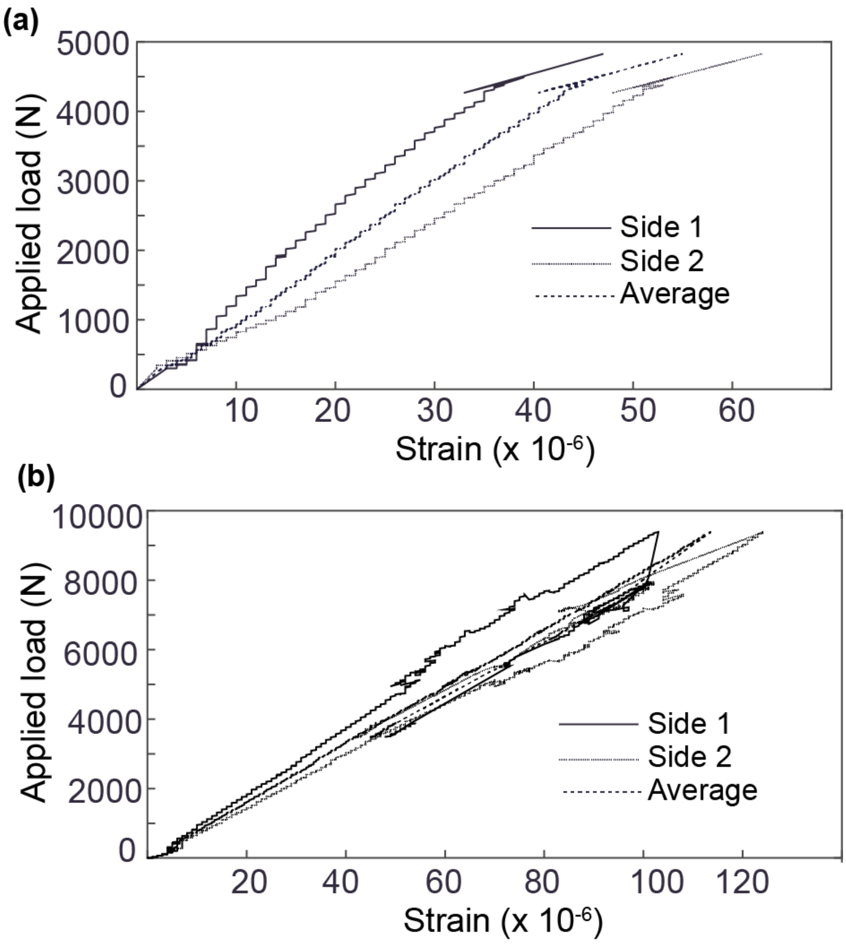

Figure 10: Applied load–middle region longitudinal strain relationships in (a) reference annealed glass-bolted joints and (b) reinforced annealed glass-bolted joints

5.2. Heat-strengthened glass-bolted joints test specimens

5.2.1. Reference (i.e. unreinforced) heat-strengthened glass-bolted joints test specimens

Reference (i.e. unreinforced) heat-strengthened glass–bolted joints showed qualitatively very similar load response and failure behaviour to that of the reference annealed glass specimens. The joints failed due to a complete fracture across the entire width of the glass specimens in the joint area, whereas middle regions of the glass specimens were undamaged. However, as expected, the load capacity of the heat-strengthened glass-bolted joint (~5960 N) (dotted line in Fig. 11) was higher compared to that of the reference annealed glass specimen (~3920 N) (reported maximum load for other two heat-strengthened glass reference bolted joints were 5700 N and 6120 N) (average maximum load – 5927 N). One glass specimen fractured at applied load ~5960 N and the second glass specimen briefly resisted the increasing load before the complete brittle joint failure at applied load ~6200 N (Fig. 11).

5.2.2. Reinforced heat-strengthened glass-bolted joint test specimens

The load response and the failure behaviour of the reinforced heat-strengthened glass-bolted joints were qualitatively similar to that of the reinforced annealed glass (Section 5.1.2). The solid lines in Fig. 11 shows the reported load response of the reinforced heat-strengthened glass test specimens. The reinforced joints showed a higher load capacity (~12000 N (reported maximum load for other two heat-strengthened glass reinforced bolted joints were 11200 N and 12300 N – average maximum load – 11833 N) compared to ~5960 N of the reference joint) and a delayed failure behaviour, albeit a significant drop in the load resistance due to the fracture of glass, similar to that of the reinforced annealed glass-bolted joints. The GFRP strip contributed to resist the applied load after the glass has cracked in the vicinity of the bolted joints.

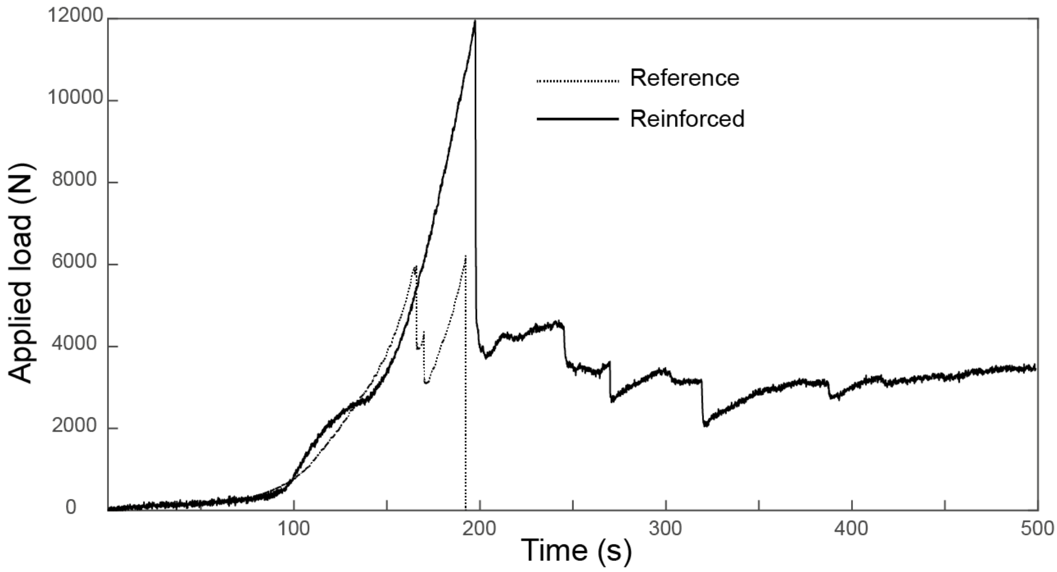

Figure 11: Heat strengthened glass-bolted joints: Load-time relationships of the reference and reinforced joints

5.3. Tempered glass glass-bolted joints test specimens

5.3.1. Reference (i.e. unreinforced) tempered glass-bolted joints test specimens

Reference tempered glass-bolted joint test specimens were tested in the same way as the reference annealed and heat-strengthened glass-bolted test specimens. Unlike other reference test specimens (Section 5.1.1 and 5.2.1) where glass only failed across the bolted joint, the tempered glass specimens failed fully where glass shattered into small dices at once with no unbroken glass (see Fig. 12a). The load response (the dotted line in Fig. 12b) suggests the load capacity of the reference tempered glass-bolted joint test specimen was ~14120 N, a significantly higher load capacity compared to other glass specimens (reported maximum load for other two reference tempered glass bolted joints were 12000 N and 14300 N) (average maximum load – 13473 N).

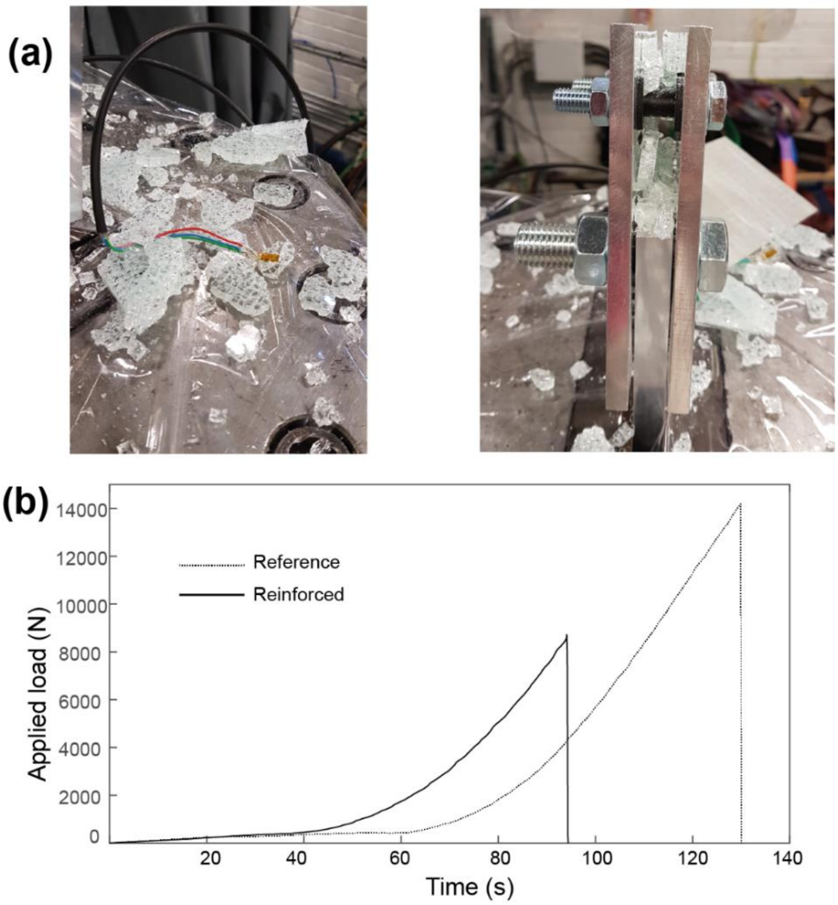

Figure 12: Tempered glass-bolted joints: (a) failure pattern of the reference joint b) load-time relationships of the reference and reinforced joints

5.3.2. Reinforced tempered glass-bolted joint test specimens

Reinforced tempered glass-bolted joints test specimens were prepared and tested in the same way as other reinforced glass-bolted joints test specimens. The solid line in Fig. 12b shows the load response of the reinforced tempered glass-bolted joints. Fig. 13 shows the test specimen after it failed. The results shown in the Fig. 12b and the visual observations during the experiment confirmed that the reinforced tempered glass specimens failed in a brittle manner similar to the reference tempered glass-bolted test specimens (Section 5.3.1). The load capacity of the reinforced test specimen (~8470 N) was lower than that of the reference specimen (~14120 N) (reported maximum load for other two reinforced tempered glass bolted tempered glass bolted joints were 8320 N and 9740 N) (average maximum load – 8843 N). All reinforced tempered glass test specimens tested in the present study failed at lower loads compared to the reference test specimens. The authors believe either possible wrinkled glass surfaces due to tempering or a high stress concentration and/or extra surface defects developed during the fabrication of the reinforced tempered glass test specimens may have caused premature failures. Detailed investigation of the surface defects after the fabrication of the joints and the mechanics of the reinforced tempered glass–bolted joints are proposed for a future study.

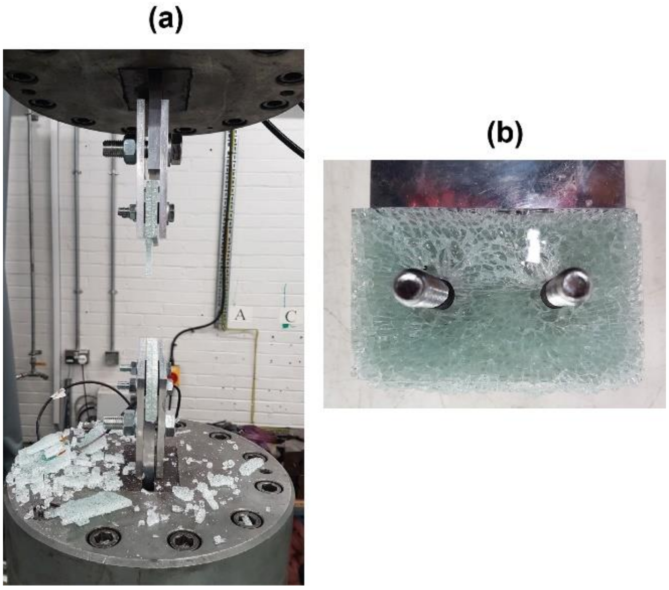

Figure 13: Reinforced tempered glass test specimen: (a) failure pattern, (b) GFRP reinforcement held broken glass pieces in the vicinity of the bolted joint

As shown in Fig.13, the GFRP strip managed to hold some broken glass pieces in the vicinity of the reinforced tempered glass-bolted joint, whereas glass completely shattered into small pieces and fully disconnected from the joints in the reference joints (Fig. 12a). However, this relatively low damage in the reinforced tempered glass specimens could be due to its lower failure load compared to the reference test specimen (i.e. less stored strain energy in the glass specimens prior to the failure).

5.4. Reference (i.e. unreinforced) laminated glass-bolted joints test specimens

Glass–bolted joints in double-layer laminated annealed glass with PVB interlayers were also tested as a reference, since laminated glass is widely used in construction industry as “structural” glass. Two-layer laminated glass specimens were used to fabricate the bolted joints in the same way as other reference joints. Fig. 14a shows the laminated glass-bolted joint test specimen prior to testing. Laminated glass test specimens too failed due to fracture of glass across the bolts (Fig. 14b). However, unlike other reference joints, the failure of the laminated glass-bolted joint was not brittle. As can be noted from the load response shown in Fig. 14c, the joint did not fail instantly after the attainment of the peak load resistance. The PVB interlayer managed to hold the broken glass pieces and ensured a notable post-cracked load resistance in the joint prior to the final failure. The peak load resistance of the laminated glass-bolted joint was ~2800 N (Fig. 14c) (reported maximum load for other two test specimens were 2670 N and 2920 N) (average maximum load – 2797 N).

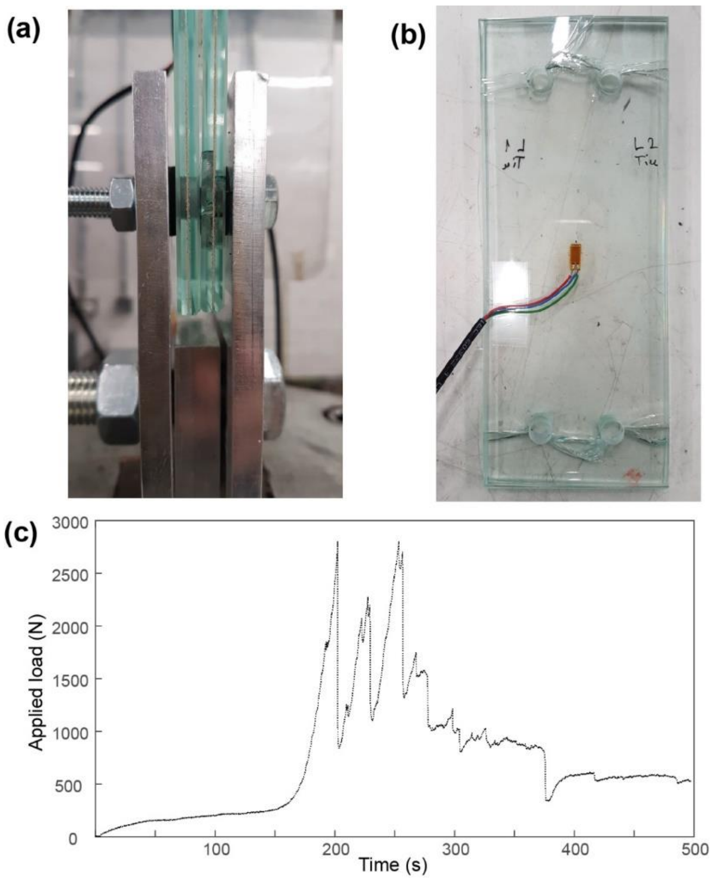

Figure 14: Reference (i.e. unreinforced) laminated annealed glass bolted joint: (a) test specimen, (b) failure pattern, (c) load-time relationship

6. Discussion: Enhanced structural performance of GFRP reinforced annealed and heat-strengthened glass-bolted joints

Fig. 15 shows the load response results of all categories of reference and reinforced glass bolted–joints test specimens investigated in the present study. All reference (i.e. unreinforced) glass–bolted joints, except in laminated-annealed glass, failed in brittle manner. As expected, the joint in the laminated glass ensured a safe failure behaviour, but its low load capacity and low post-cracked load resistance limit the structural efficiency in engineering applications. Although the tempered glass-bolted joint had the highest load capacity, lack of a post-cracked load resistance makes them less reliable for real-life applications.

The results shown in Fig. 15 suggest the enhanced structural performance of the GFRP reinforced annealed glass and heat-strengthened glass bolted joints. The maximum load resistance of ~9400 N of the reinforced annealed glass joint was ~140% and ~235% higher compared to that of the reference annealed glass (~3920 N) and laminated-annealed glass (~2800 N) test specimens, respectively. Since the laminated glass were purchased from a commercial supplier, no experiments were conducted on mechanical properties of the PVB interlayer. However, shear modulus of 1-400 MPa and shear strength up to 2 MPa were reported for commercially available PVB materials [34]. These values are low compared to those of the adhesive used to bond the GFRP strips where the shear modulus and the bond shear strength were ~2000 MPa and ~10 MPa, respectively [20].

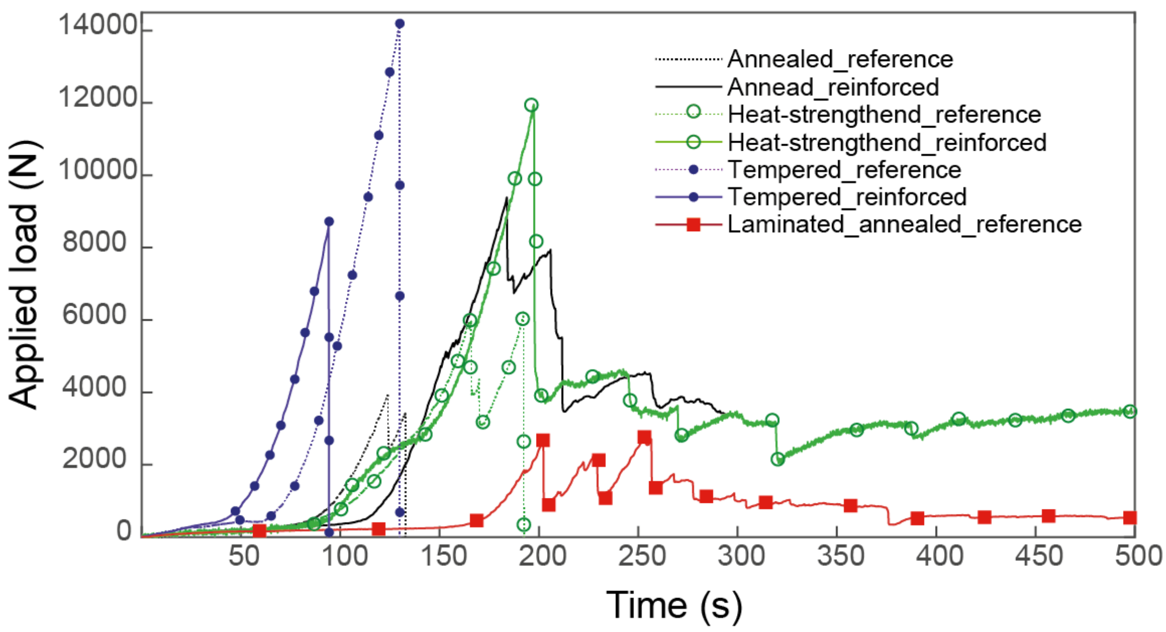

Figure 15: Load-time relationships of all categories of test specimens

Furthermore, the load capacity of the reinforced annealed glass joint (~9400 N) was ~58% higher than that of the reference joints in heat-strengthened glass (~5960 N) despite the usually superior strength properties of the latter. Just after the failure of the glass specimens, the load resistance of the reinforced annealed glass bolted joint was dropped to ~3470 N, and as can be seen from Figs. 8 and 15, the post-cracked load resistance of the joint was within the range ~3400-4570 N. This post-cracked load resistance was either higher or comparable to the peak load resistance (i.e. prior to any glass failure) of the reference annealed (~3920 N) and laminated glass (~2800 N) joints. The post-cracked load resistance of the reinforced annealed glass joint was significantly higher compared to that of ~350-1750 N of the joints in laminated glass.

The maximum load resistance of ~12000 N of the reinforced heat-strengthened glass joint was ~100% higher compared to that of the reference unreinforced glass test specimen (~5960 N). The load resistance of the reinforced heat-strengthened joint was dropped to ~3800 N (see Figs. 11 and 15) after the failure of the glass. This drop from the peak load (i.e. to ~3800 N from 12000 N) was higher compared to that of the reinforced annealed glass (i.e. to ~3470 N from ~9400 N). The large drop in the load resistance up on cracking of the glass may be due to the more significant cracking occurred in the reinforced heat-strengthened glass compared to that in the reinforced annealed glass as a result of higher strain energy stored in the former (i.e. 12000 N load resistance compared to ~9400 N load resistance) and the high initial residual stress in heat-strengthened glass. Nevertheless, the post-cracked load resistance of the reinforced heat-strengthened glass joint ~2200-4600N was comparable to that of reinforced annealed glass joints (~3400-4570 N), and it was significantly higher compared to that of ~350-1750 N of the joints in laminated-annealed glass.

The results suggest the enhanced load capacity and an ability to resist the applied load after the fracture of glass in reinforced glass-bolted joints in annealed and heat-strengthened glass. As summarised in Table 4, the peak load capacity and the post-cracked load resistance of the reinforced joints were significantly higher compared to those of the equivalent joints in commercially available laminated glass. Although, the peak load resistance of the reinforced joints in annealed and heat-strengthened glass were somewhat lower than that of tempered glass-bolted joints, the notable post-cracked load resistance characteristics of the reinforced annealed and heat-strengthened glass joints make them better options in practical engineering applications compared to the bolted joints in tempered glass, which has no post-fracture load resistance.

Table 4: The peak load capacity and the post-cracked load resistance of the reinforced bolted joints in annealed and heat-strengthened glass

Reinforced Joint – Glass type	Peak load (N)	Post-cracked load resistance (N)	% increase in the peak load compared to the reference (i.e. unreinforced) joint	% increase in the peak load compared to the joint in laminated glass	% increase in the post-cracked load resistance compared to the joint in laminated glass
Annealed	9400	3400-4570	~140	~235	~280
Heat-strengthened	12000	2200-4600	~100	~330	~225

7. Conclusions

The experimental results of the double-lap glass-bolted tension joint test specimens showed annealed, heat-strengthened and tempered glass failed in brittle matter due to glass fracture. On the other hand, bolted joints in laminated annealed glass showed some post-cracked load resistance after the glass has cracked in the vicinity of the bolted joints.

The results showed that the use of adhesively bonded GFRP strips as a means of reinforcing annealed and heat-strengthened glass in the vicinity of the bolted joints significantly enhanced the peak load capacity of the joints compared to the respective reference (i.e. unreinforced) glass-bolted joints. Furthermore, the post-cracked load resistance of the GFRP reinforced annealed and heat-strengthened glass bolted joints were significantly higher compared to that of similar bolted joints in commercially available laminated-annealed glass. Despite the GFRP reinforcement ensured better structural performance of the bolted joints in annealed and heat-strengthened glass, the technique did not enhance the structural performance of tempered glass–bolted joints.

A future study on the effectiveness of the proposed GFRP reinforcement technique under other loading scenarios such as compression, in-plane and out-of-plane bending loading cases and a detailed design of the GFRP reinforcement is proposed as a means of ensuring real-life practical applications of the concept proposed in the present paper. A detailed experiment and computational investigation based on strain/displacement evolution, likely failure modes and dynamic/fatigue behaviour of the proposed joint technology will be required for the development of a comprehensive design methodology for GFRP reinforced glass-bolted joints configurations. The effectiveness of the proposed GFRP reinforcement technique under environmental ageing, including elevated temperature, should also be considered in order to evaluate the benefits in real-life structures.

Data access statement

All data supporting this study are openly available from the University of Southampton repository at https://doi.org/10.5258/SOTON/D1044.

Acknowledgements

Funding received from the Institution of Structural Engineers (IStructE) MSc Research Grants 2016/17 is gratefully acknowledged.

References

[1] Young CH, Chen YL, Chen PC. Heat insulation solar glass and application on energy efficiency buildings. *Energy and Buildings* 2014; 78: 66-78

[2] Haldimann M, Luible A, Overend M. Structural use of glass. Zurich: *International Association for Bridge and Structural Engineering*, 2008.

[3] Santarsiero M, Louter C, Nussbaumer A. Laminated connections for structural glass components: a full-scale experimental study. *Glass Structures an Engineering* 2017; 2, 79–101.

[4] Katsivalis I, Thomsen O, Feih S, Achintha M. Strength evaluation and failure prediction of bolted and adhesive glass/steel joints. *Glass Structures and Engineering* 2018; 3(2): 183–196.

[5] Firmo JP, Roquette MG, Correia JR, Azevedo AS. Influence of elevated temperatures on epoxy adhesive used in CFRP strengthening systems for civil engineering applications. *International Journal of Adhesion and Adhesives* 2019; 93: 102333

[6] Bedon C, Santarsiero M. Transparency in Structural Glass Systems Via Mechanical, Adhesive, and Laminated Connections – Existing Research and Developments. *Adv. Eng. Mater.* 2018. 20(5): 1700815.

[7 Bernard F, Daudeville L. Point fixings in annealed and tempered glass structures: Modeling and optimization of bolted connections. *Eng. Struct.* 2009 31(4): 946–955.

[8] IStructE. Structural use of glass in buildings. 2nd ed. London: The Institution of Structural Engineers, 2014.

[9] Watson J, Nielsen J, Overend M. A critical flaw size approach for predicting the strength of bolted glass connections. Eng. Struct. 2013; 57: 87–99.

[10] Achintha M. Sustainability of glass in construction. In: Khatib J, editor. Sustainability of Construction Materials (2nd ed.), Woodhead Publishing, United Kingdom (2016), pp. 79-104.

[11] Balan B, Achintha M. Assessment of stresses in float and tempered glass using Eigenstrains. Exp. Mech. 2015; 55(7):1301-15.

[12] Nielsen JH, Olesen JF, Stang H. Characterization of the Residual Stress State in Commercially Fully Toughened Glass. J. Mater. Civil Eng. 2010; 22(2):179-85.

[13] Baitinger M, Feldmann M. Design concept for bolted Glass. In: Proceedings of Challenging Glass 2 Conference. Delft, May 2010. p. 237-246.

[14] Ledbetter SR, Walker AR, Keiller AP. Structural Use of Glass. J. Architect. Eng. 2006; 12(3) 137-149.

[15] Achintha M, Bessonov M. A novel design concept for connections in glass: structural integrity of glass reinforced with externally-bonded GFRP laminates. In: Proceedings of IABSE conference Creativity and Collaboration, Bath, April 2017. p. 45-46.

[16] Achintha M, Zirbo T. (2018). Developments in GFRP reinforced bolted joints in glass. In C. Louter, F. Bos, & J. Belis (Eds.), Challenging Glass Conference Proceedings (Vol. 6). Delft University of Technology May 2018. P. 291-298.

[17] Syed AK, Fitzpatrick ME, Moffatt JE, Doucet J, Durazo-Cardenas I. Effect of impact damage on fatigue performance of structures reinforced with GLARE bonded crack retarders. *International Journal of Fatigue* 2015; 80:231-237.

[18] Achintha M, Balan B. An experimentally validated contour method/eigenstrains hybrid model to incorporate residual stresses in glass structural designs. *J Strain Anal Eng Des.* 2015; 50:614–27.

[19] SCALP Instruction Manual, ver 5.0, GlassStress Ltd., Tallinn, Estonia (2015).

[20] Achintha M, Balan B. Mechanical prestressing of annealed glass beams using pretensioned GFRP: characterisation and potentiality. *Structures*, 2019; 20:11-19.

[21] Aben H, Guillemet C. Photoelasticity of Glass. Berlin: Springer. 1993.

[22] Aben H, Anton J, Errapart A. Modern photoelasticity for residual stress measurement in glass. *Strain* 2008; 44:40-48.

[23] Narayanaswamy OS. A model of structural relaxation in glass. *Journal of the American Ceramic Society* 1971; 54: 491-498.

[24] BS EN 1863-1 2011. Glass in building. Heat strengthened soda lime silicate glass. Definition and description, London: BSI.

[25] BS EN 12150-1: 2015+A1:2019. Glass in buildings. Thermally toughened soda lime silicate safety glass. Definition and description, London: BSI.

[26] Technical data sheet product: EL2 Epoxy Laminating Resin, Easycomposites, 2015, p. 2.

[27] Achintha M, Balan B. Characterisation of the mechanical behaviour of annealed glass–GFRP hybrid beams. *Construction and Building Materials* 2017; 147: 174-184.

[28] Araldite2020. Product sheet. Basel, Switzerland: Huntsman Advanced Materials; 2015.

[29] ASTM D638-02. Standard test method for tensile properties of plastics. United States: ASTM International; 2002.

[30] Draganić H, Dokšanović T, Markulak D. Investigation of bearing failure in steel single bolt lap connections. *Journal of Constructional Steel Research* 2014; 98:59-72.

[31] Gerendt C, Dean A, Mahrholz T, Rolfes R. On the progressive failure simulation and experimental validation of fiber metal laminate bolted joints. *Composites Structures* 2019; 229:111368.

[32] Dean A, Asur Vijaya Kumar PK, Reinoso J, Gerendt C, Paggi M, Mahdi E, Rolfes R. A multi-phase-field fracture model for long fiber reinforced composites based on the Puck theory of failure. *Composites Structures* 2020; 251:112446.

[33] Veer FA, Louter C, Bos F P. The strength of annealed, heat-strengthened and fully tempered float glass. *Fatigue & Fracture of Engineering Materials & Structures* 2009: 32:18-25.

[34] Zhang X, Hao H, Shi Y, Cui J. The mechanical properties of Polyvinyl Butyral (PVB) at high strain rates. *Construction and Building Materials* 2015; 93:404-415.